Title: Data to support Activating a High-Spin Iron(II) Complex to Thermal Spin-Crossover with an Inert Non-Isomorphous Molecular Dopant

Creator(s): Malcolm A. Halcrow,[1] Hari Babu Vasili,[1] Christopher M. Pask,[1] Alexander N. Kulak[1] and Oscar Cespedes[1]

Organisation(s): 1. University of Leeds, UK.

Publication Year: 2024

Description: $[Fe(bpp)_2][ClO_4]_2$ (bpp = 2,6-bis{pyrazol-1-yl}pyridine; monoclinic, *C*2/*c*) is high-spin between 5-300 K, and crystallises with a highly distorted molecular geometry that lies along the octahedral−trigonal prismatic distortion pathway. In contrast, $[Ni(bpp)_2][ClO_4]_2$ (monoclinic, $P2_1$) adopts a more regular, near-octahedral coordination geometry. Slowly crystallised solid solutions $[Fe_xNi_{1-x}(bpp)_2][ClO_4]_2$ with x = 0.53 (**1a**) and 0.74 (**2a**) adopt the $P2_1$ lattice, while x = 0.87 (**3a**) and 0.94 (**4a**) are mixed-phase materials with the high-spin *C*2/*c* phase as the major component. These materials exhibit thermal spin-transitions at $T_{½}$ = 250 ±1 K which occurs gradually in **1a**, and abruptly and with narrow thermal hysteresis in **2a**-**4a**. The transition proceeds to 100 % completeness in **1a** and **2a**; that is, the 26 % Ni doping in **2a** is enough to convert high-spin $[Fe(bpp)_2][ClO_4]_2$ into a fully SCO-active material. Rapidly precipitated powders with the same compositions behave similarly, but contain a fraction of amorphous material in addition to the two crystal phases when x ≥ 0.74.

Cite as: Halcrow, Malcolm A., Vasili, Hari Babu, Pask, Christopher M., Kulak, Alexander N., and Cespedes, Oscar (2024). Data to support Activating a High-Spin Iron(II) Complex to Thermal Spin-Crossover with an Inert Non-Isomorphous Molecular Dopant. University of Leeds. [Dataset] https://doi.org/10.5518/1493

Related publication: Halcrow, Malcolm A., Vasili, Hari Babu, Pask, Christopher M., Kulak, Alexander N., and Cespedes, Oscar (2024). Activating a High-Spin Iron(II) Complex to Thermal Spin-Crossover with an Inert Non-Isomorphous Molecular Dopant. *Dalton Transactions*, doi: 10.1039/d4dt00443d.

Contact: m.a.halcrow@leeds.ac.uk

2. TERMS OF USE

3. PROJECT AND FUNDING INFORMATION

n/a

4. CONTENTS

The dataset contains data for this study:

Elemental microanalyses (*microanalysis.zip*).

Scanning Electron Microscopy images and EDX element maps (*EDX*.zip)

X-ray powder diffraction data (measured and simulated – *XRPD*.zip).

Solid state magnetic susceptibility measurements (raw and processed data – *SQUID*.zip).

X-ray Crystallographic data (*crystal*.zip):

- Structure of $[Ni(bpp)_2][ClO_4]_2$ at 120 K (CCDC 2332656)
- Structure of $[Fe(bpp)_2][ClO_4]_2$ at 300 K (CCDC 2332657)
- Structure of $[Fe(bpp)_2][PF_6]_2$ at 300 K (CCDC 2332658)
- Structure of **1a** at 300 K (CCDC 2332659)
- Structure of **1a** at 100 K (CCDC 2332660)
- Structure of **2a** at 100 K (CCDC 2332661)
- Variable temperature unit cell data for **1a**
- Variable temperature unit cell data for **2a**

Density functional theory (DFT) calculations (*SPARTAN* files – *DFT*.zip).

5. METHODS

Full details are provided in the related publication, listed above.

Compounds referred to in this dataset

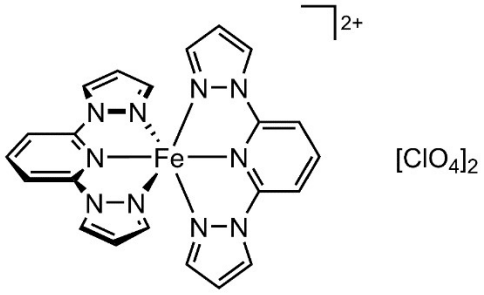

$[Fe(bpp)_2][ClO_4]_2$
Bis[di(pyrazol-1-yl)pyridine]iron(II) diperchlorate
$C_{22}H_{18}Cl_2FeN_{10}O_8$

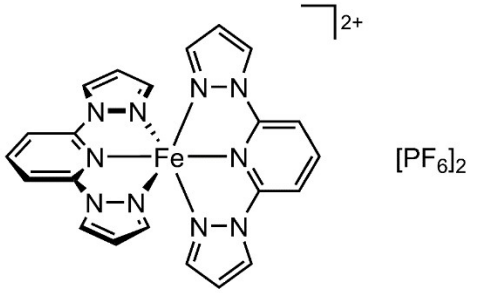

$[Fe(bpp)_2][PF_6]_2$
Bis[di(pyrazol-1-yl)pyridine]iron(II) di(hexafluorophosphate)
$C_{22}H_{18}F_{12}FeN_{10}P_2$

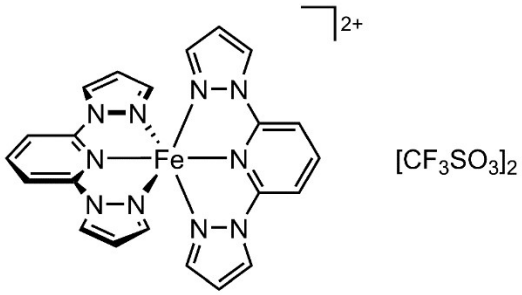

$[Fe(bpp)_2][CF_3SO_3]_2$
Bis[di(pyrazol-1-yl)pyridine]iron(II) di(trifluoromethanesulfonate)
$C_{24}H_{18}F_6FeN_{10}O_6S_2$

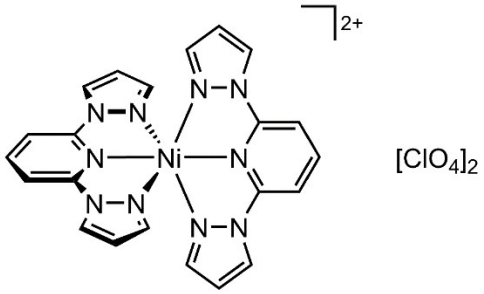

$[Ni(bpp)_2][ClO_4]_2$
Bis[di(pyrazol-1-yl)pyridine]nickel(II) diperchlorate
$C_{22}H_{18}Cl_2N_{10}NiO_8$

Compounds referred to in this dataset (continued)

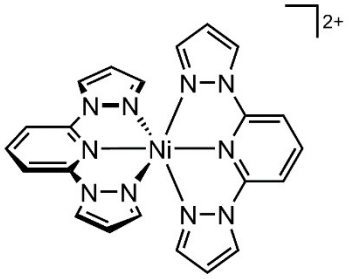

$[Ni(bpp)_2][PF_6]_2$
Bis[di(pyrazol-1-yl)pyridine]nickel(II) di(hexafluorophosphate)
$C_{22}H_{18}F_{12}N_{10}NiP_2$

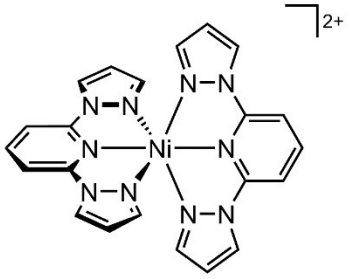

$[Ni(bpp)_2][CF_3SO_3]_2$
Bis[di(pyrazol-1-yl)pyridine]nickel(II) di(trifluoromethanesulfonate)
$C_{24}H_{18}F_6N_{10}NiO_6S_2$

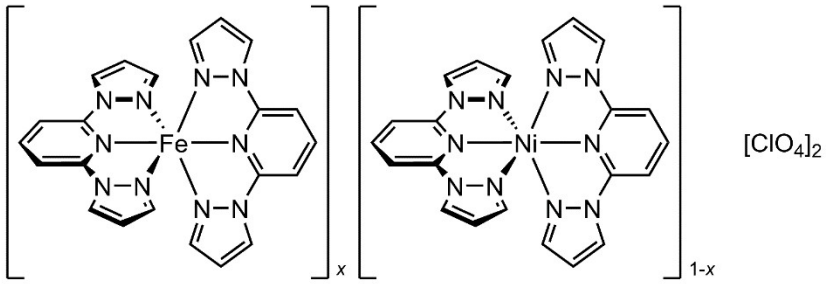

$[Fe_xNi_{1-x}(bpp)_2][ClO_4]_2$
Bis[di(pyrazol-1-yl)pyridine]iron(II):nickel(II) diperchlorate solid solution
$C_{22}H_{18}Cl_2Fe_xN_{10}Ni_{1-x}O_8$
x = 0.53 (slowly crystallised), **1a**
x = 0.52 (rapidly precipiated), **1b**
x = 0.74 (slowly crystallised), **2a**
x = 0.74 (rapidly precipiated), **2b**
x = 0.87 (slowly crystallised), **3a**
x = 0.88 (rapidly precipiated), **3b**
x = 0.94 (slowly crystallised), **4a**
x = 0.93 (rapidly precipiated), **4b**

Complex cations studied by DFT calculations

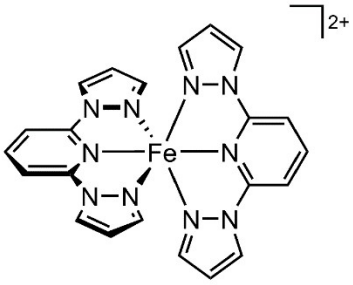

$[Fe(bpp)_2]^{2+}$
Bis[di(pyrazol-1-yl)pyridine]iron(II)
$C_{22}H_{18}FeN_{10}$

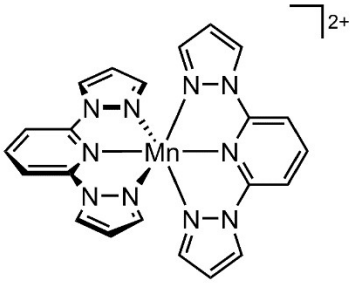

$[Mn(bpp)_2]^{2+}$
Bis[di(pyrazol-1-yl)pyridine]manganese(II)
$C_{22}H_{18}MnN_{10}$

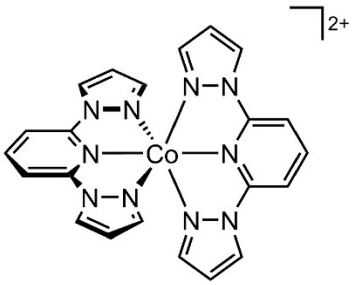

$[Co(bpp)_2]^{2+}$
Bis[di(pyrazol-1-yl)pyridine]cobalt(II)
$C_{22}H_{18}CoN_{10}$

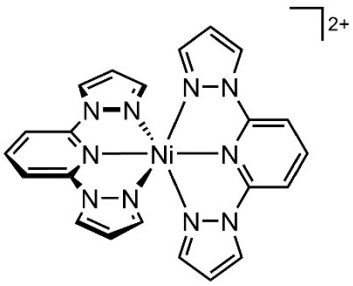

$[Ni(bpp)_2]^{2+}$
Bis[di(pyrazol-1-yl)pyridine]nickel(II)
$C_{22}H_{18}N_{10}Ni$

Complex cations studied by DFT calculations (continued)

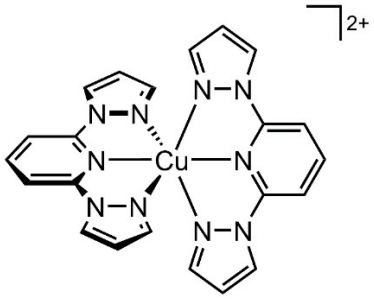

$[Cu(bpp)_2]^{2+}$
Bis[di(pyrazol-1-yl)pyridine]copper(II)
$C_{22}H_{18}CuN_{10}$

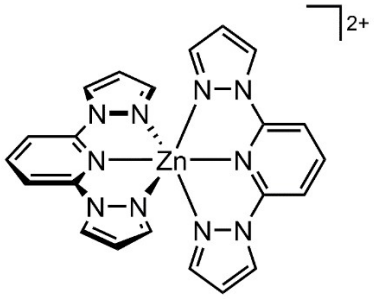

$[Zn(bpp)_2]^{2+}$
Bis[di(pyrazol-1-yl)pyridine]zinc(II)
$C_{22}H_{18}N_{10}Zn$

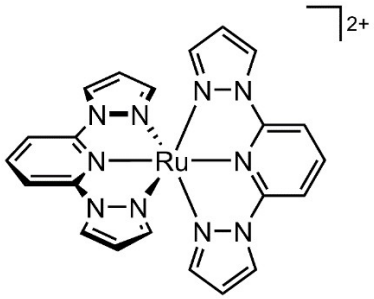

$[Ru(bpp)_2]^{2+}$
Bis[di(pyrazol-1-yl)pyridine]ruthenium(II)
$C_{22}H_{18}N_{10}Ru$